International Journal of Pharmaceutics 403 (2011) 73–82

Contents lists available at ScienceDirect

International Journal of Pharmaceutics

journal homepage: www.elsevier.com/locate/ijpharm

Sodium carboxymethylcellulose scaffolds and their physicochemical effects on partial thickness wound healing

Nor Amlizan Ramli [a,b], Tin Wui Wong [a,b,*]

[a] Non-Destructive Biomedical and Pharmaceutical Research Centre, Universiti Teknologi MARA, 42300, Puncak Alam, Selangor, Malaysia
[b] Particle Design Research Group, Faculty of Pharmacy, Universiti Teknologi MARA, 42300, Puncak Alam, Selangor, Malaysia

ARTICLE INFO

Article history:
Received 1 September 2010
Received in revised form 5 October 2010
Accepted 15 October 2010
Available online 23 October 2010

Keywords:
Sodium carboxymethylcellulose
Transepidermal water loss
Wound dressing
Wound healing

ABSTRACT

This study investigated critical physicochemical attributes of low (LV), medium (MV) and high molecular weight (HV) sodium carboxymethylcellulose (SCMC) scaffolds in partial thickness wound healing. SCMC scaffolds were prepared by solvent-evaporation technique. Their *in vitro* erosion, moisture affinity, morphology, tensile strength, polymer molecular weight and carboxymethyl substitution, and *in vivo* wound healing profiles were determined. Inferring from rat wound size, re-epithelialization and histological profiles, wound healing progressed with HV scaffold > LV–MV scaffold > control with no scaffold. The transepidermal water loss (TEWL) from wound of rats treated by control > HV scaffold > LV–MV scaffold. HV scaffold had the highest tensile strength of all matrices and was resistant to erosion in simulated wound fluid. In spite of constituting small nanopores, it afforded a substantial TEWL than MV and LV scaffolds from wound across an intact matrix through its low moisture affinity characteristics. The HV scaffold can protect moisture loss without its excessive accumulation at wound bed which hindered re-epithelialization process. Regulation of transepidermal water movement and wound healing by scaffolds was governed by SCMC molecular weight instead of its carboxymethyl substitution degree or matrix pore size distribution, with large molecular weight HV preferred over lower molecular weight samples.

1. Introduction

Sodium carboxymethylcellulose (SCMC) is a sodium salt of carboxymethyl ether cellulose. It is synthesized by swelling cellulose with sodium hydroxide and alkali-catalyzed reaction of cellulose with chloroacetic acid (Sudhakar et al., 2006). The degree of ether substitution of carboxymethylcellulose, defined as number of hydroxyl groups substituted by anhydroglucose unit, varies between 0.60 and 1.00 in grades for pharmaceutical application (Sebert et al., 1994). Its molecular weight, on the other hand, can range from 90,000 to 2,000,000 g/mol (Kulicke et al., 1996; Sudhakar et al., 2006). SCMC has been widely employed as viscosity modifier, emulsifier, stabilizer and lubricant in the development of pharmaceutical dosage forms (Guo et al., 1998; Ludwig, 2005; Sudhakar et al., 2006). The rheological profile of carboxymethylcellulose is found to be largely affected by molecular weight of the polymer chains instead of degree of substitution of cellulose structure (Kulicke et al., 1996).

Carboxymethycellulose has a high water bonding capacity, good compatibility with skin and mucous membrane, is physiologically harmless and available abundantly at a low price (Kulicke et al., 1996; Liu et al., 2007; Ludwig, 2005; Sudhakar et al., 2006). These attributes render it suitable for use as matrix polymer for wound dressing. Over the years, SCMC has been utilized as the sole material or in combination with drug and co-excipients in wound dressing for the treatment of partial thickness wound, deep diabetic foot ulcer, pressure sore, surgical wound, toxic epidermal necrolysis, and as dermal filler (Caruso et al., 2004; D'Hemecourt et al., 1998; Huang and Yang, 2008; Huang et al., 2010; Kamer et al., 2008; Liu et al., 2007; Piaggesi et al., 2001; Vloemans et al., 2001; Wang et al., 2007; Williams, 1999). Drugs such as silver and co-excipients such as hyaluronic acid, poly(*N*-vinyl pyrrolidone), gelatin, pectin or propylene glycol have been used in formulation of SCMC-based dressings. These wound dressings are available in the form of sponge, hydrogel, hydrofibre or membrane. In formulation complexing with co-excipients, toxic reagent or organic solvent is applied in parts of the fabrication process. Additional purification steps, flame-proof facility and solvent recovery equipment are needed thereby increasing the cost of product.

In the absence of drug or co-excipient, pure SCMC dressing has found its application in partial thickness burn, leg ulcer, surgical wound and pressure sore through providing warm, moist local wound conditions for optimum healing (D'Hemecourt et al., 1998;

* Corresponding author at: Faculty of Pharmacy, Universiti Teknologi MARA, 42300, Puncak Alam, Selangor, Malaysia.
Tel.: +60 3 32584691; fax: +60 3 32584602.
E-mail address: wongtinwui@salam.uitm.edu.my (T.W. Wong).

0378-5173/$ – see front matter © 2010 Elsevier B.V. All rights reserved.
doi:10.1016/j.ijpharm.2010.10.023

Piaggesi et al., 2001; Vloemans et al., 2001; Williams, 1999). Pure SCMC dressing, in spite of being drug free, does not negatively impact but instead it promotes wound healing with good tolerance similar to drug loaded dressing. In comparison to allograft skin, pure SCMC dressing is a simpler and safer alternative. The sourcing of allograft skin can be difficult. The skin may be a bed for disease transmission and is often met with poor religion or social acceptance. Nonetheless, it is not known if the reported SCMC dressing represents the best drug-free matrix for wound healing. The moisture diffusion can be governed by pore size distribution of a matrix (Karathanos and Saravacos, 1993). The pore characteristics of a matrix can affect the moisture protection capacity of a dressing. There is no research study hitherto examining the relationship between construct of SCMC dressing and its wound healing capacity. Similar comments have been made by Czaja et al. (2006) on membrane prepared from microbial cellulose. As such, the present study aims to investigate the physicochemical attributes of SCMC scaffolds and their effects on moisture protection and healing using partial thickness wound as the model injury.

2. Materials and methods

2.1. Materials

High molecular weight SCMC (HV, Sigma–Aldrich Chemie, Netherlands), medium molecular weight SCMC (MV, Sigma–Aldrich Chemie, Germany) and low molecular weight SCMC (LV, Sigma–Aldrich Chemie, Germany) were employed as matrix polymers of scaffolds. Other chemicals employed in this study included disodium hydrogen orthophosphate anhydrous (Fischer Scientific, UK) and sodium hydroxide (Merck, Germany) for the preparation of buffer, sodium chloride (Merck, Germany) for the preparation of wound cleansing solution, sodium azide (Merck, Germany) and dextran (Sigma–Aldrich Chemie, Germany) for gel permeation chromatography analysis, Haeris haematoxylin (VWR International, UK), eosin (Microm International, Germany), picric acid (Sigma–Aldrich Chemie, Germany), fuchsin acid (Ajax Finechem, Australia), hexane (Merck, Germany), ethanol (Merck, Germany) and xylene mixtures of isomers with dibutylftalan (VWR International, UK) for histology study, and ketamine hydrochloride and xylazine hydrochloride (Troy Laboratories, Australia) as anaesthetic agents.

2.2. Preparation of SCMC scaffold

2% (w/w) SCMC suspension was left for hydration for at least 6 h at 25.0 ± 1.0 °C under continuous magnetic stirring at 150 ± 1 rpm. Fifty gram of air bubble-free and hydrated polymer solution were then transferred into a glass petri dish (internal diameter = 9 cm), similar to a protocol adopted by Ashikin et al. (2010). The solution was left to hot air drying in the oven (Memmert, Germany) at 40.0 ± 0.5 °C for 5 days. The dried scaffold was shaped into circular matrices with a diameter of 22 mm, an average weight of 0.05 ± 0.01 g and an average thickness of 0.127 ± 0.010 mm by a stainless steel moulding system. The circular shaped samples were conditioned in desiccators prior to tests. At least triplicates were carried out for each scaffold formulation.

2.3. Erosion and water uptake

The analysis of scaffold erosion and water uptake capacity was conducted by immersing an accurately weighed scaffold with known size in a glass lid-covered petri dish containing 20 ml USP phosphate buffer pH 7.4 (sink condition simulating the pH of wound bed) and incubated at 37.0 ± 0.2 °C (Memmert, Germany) for a duration of 12 h. At specific intervals, the weight of scaffold was characterized after removing its surface moisture through running the scaffold gently over a dry petri dish till no sign of moisture left on the immediate dish surface contacted by scaffold. The scaffold was then oven-dried at 40.0 ± 0.5 °C for 5 days and subsequently equilibrated to a constant weight by storing in a desiccator at 25.0 ± 1.0 °C.

The erosion (E_I) and water uptake (WU_I) indices of scaffold were defined as:

$$E_I = \frac{W_i - W_{t(d)}}{W_i} \times 100\% \quad (1)$$

where W_i = initial dry scaffold weight and $W_{t(d)}$ = dry weight of scaffold collected at time, t.

$$WU_I = \frac{W_t - W_{t(d)}}{W_{t(d)}} \times 100\% \quad (2)$$

where W_t = wet weight of scaffold at t.

Ten replicates were conducted and the results averaged.

2.4. Moisture content

The moisture content of a scaffold was determined using skin hydration measurement device (Corneometer® CM825, Cologne, Germany) as previously reported (Anuar et al., 2007; Wong et al., 2007). Triplicates were conducted and the results averaged.

2.5. Moisture adsorption

An accurately weighed scaffold (W_i) was placed on a petri dish located in a weighing microbalance (Sartorius AG, Germany) with its relative humidity maintained at 90.0 ± 2.0% by means of deionized water. The weight changes of scaffold (W_t) were recorded at specified intervals over a period of 5 h at 25.0 ± 2.0 °C. The moisture adsorption capacity (MAC) of scaffold was defined by the following equation:

$$MAC = \frac{W_t - W_i}{W_i} \times 100\% \quad (3)$$

Triplicates were conducted and the results averaged.

2.6. Surface and cross-sectional morphology

The surface and cross-sectional structures of a scaffold were examined using the field emission scanning electron microscopy technique (JSM-6360LA, JEOL, Japan). The scaffold was fixed with a carbon tape onto studs without prior treatment in examination of surface structure, and with prior freeze cutting using the liquid nitrogen at −196 °C in case of elucidating its cross-sectional morphology. The prepared studs were platinum-coated and viewed directly under a scanning electron microscope at an accelerating voltage of 1 kV. The morphological images of scaffold were captured using low emission imaging detector mode. Representative sections were photographed.

2.7. Molecular weight

The molecular weight of SCMC for use in scaffold fabrication was determined using a gel permeation chromatography technique (1100 series, Agilent Technologies, Germany) by means of a refractive index detector as previously reported by Ashikin et al. (2010). PL aquagel-OH mixed column (7.5 × 300 mm; 8 μm; Agilent Technologies, United Kingdom) was used with mobile phase consisted of 0.1% (w/w) sodium azide dissolved in deionised water. The flow rate of mobile phase and column temperature was kept at 0.5 ml/min and 30 °C respectively. Dextrans with molecular

weights of 50,000, 80,000, 150,000, 270,000, 410,000, 670,000 and 1,400,000 Da were used as standards. 10 mg/ml of sample solution was filtered through a cellulose nitrate membrane (pore diameter = 0.45 μm, Sartorius, Germany) before analysis. At least triplicates were conducted and the results averaged.

2.8. Fourier transform infra-red spectroscopy study

A total of 2.5% (w/w) of sample, with respect to potassium bromide (KBr) disc, was mixed with dry KBr (FTIR grade, Aldrich, Germany). The mixture was ground into a fine powder using an agate mortar before compressing into a disc. Each disc was scanned at a resolution of 4 cm^{-1} over a wavenumber region of 400–4000 cm^{-1} using a FTIR spectrometer (Spectrum 100 FTIR system, Perkin Elmer, USA). The characteristic peaks of IR transmission spectra were recorded. The substitution degree of carboxymethyl moiety on SCMC was calculated from the quotient of absorbance values at 1601.3–1625.3 cm^{-1} to 3262.2–3436.9 cm^{-1} of which denoted C=O of carboxymethyl moiety to O–H functional group of the main SCMC chain. A higher absorbance quotient value represented a higher degree of carboxymethyl moiety substitution. At least triplicates were conducted and the results averaged.

2.9. Wound healing study

Healthy male Sprague Dawley rats (Genetic Improvement and Farm Technologies Sdn Bhd, Malaysia), aged 3 months and weighed 200 ± 20 g, were acclimatized for 7 days in individual housing under 12 h light/dark cycle with deionized water and animal feed given *ad libitum*. The ambient temperature was set at 25.0 ± 2.0 °C with relative humidity maintained at 55.0 ± 2.0% in automated caging system installed with HEPA filter system (Techniplast, Italy) and subjected to daily 70% (w/w) ethanolic solution swap. The rats were randomly divided into 12 per group as control, animals receiving LV, MV and HV scaffolds.

The wounding of animal proceeded at day 8 with anaesthesia being first induced by means of an intramuscular injection of ketamine and xylazine at 90 mg/kg and 10 mg/kg body weight of rodent respectively. Subsequently, the hair at dorsal region was removed using a sharp blade and the shaved area was cleansed with alcohol swab. The contact partial thickness wound was produced on the shaved dorsal region of each rat using deionised water heated to 65.0 ± 5.0 °C through placing 6 ml of water in a circular plastic ring (internal diameter = 1.27 cm; external diameter = 2.20 cm) secured onto the shaved region of rat by an adhesive agent for 1 min in 9 repetitive cycles. Following the wound induction, the scaffold was applied onto the wounded area with the aid of standard gauze and 3 M adhesive tape. The control rats were defined as animals with no dressing applied. All experiments were conducted in accordance to institutional ethics policy adapting the international guidelines (OECD Environment, Health and Safety).

2.10. Wound morphology

The surface morphology of wound was recorded using a digital camera (Olympus μ720 SW, Olympus, Japan) at specific intervals of healing process in the absence of scaffold. The size of wound was determined using the digital micrometer (Mitutoyo, Japan). Re-epithelialization was inferred from the size profile of wound as described by the following equation:

$$\text{Percentage re-epithelialization} = \frac{(\text{Wound size at } t = 0) - (\text{Wound size at } t)}{\text{Wound size at } t = 0} \times 100\% \quad (4)$$

where the wound size was an average measurement from the longest and shortest dimensions of a wounded area.

2.11. Transepidermal water loss (TEWL)

The propensity of TEWL from wound through scaffold was determined using Tewameter® TM300 attached to Cutometer 580 MPA® (Courage + Khazaka, Germany). The principle of TEWL was based upon the diffusion principle in an open chamber as described by:

$$\frac{dm}{dt} = D \times A \times \frac{dp}{dx} \quad (5)$$

where A was surface area (m^2), m was moisture transported (g), t was time (h), p was atmospheric vapour pressure (mmHg), D was diffusion constant (0.0877 g/m mmHg h) and x was distance from scaffold/skin surface to point of measurement. The measurement of TEWL was conducted under a controlled ambient relative humidity of 55.0 ± 5.0% and temperature of 25.0 ± 2.0 °C with minimal interference of air current. The probe head in contact with the test surfaces had small but constant surface area and light weight to minimize the influence of air turbulences inside the probe and unnecessary physical exertion of probe onto scaffold and wound respectively. Triplicates were conducted on each wound area and the results averaged.

2.12. Histology

Rats were sacrificed after a pre-determined period of healing. The wounded skin which included its subcutaneous tissue was collected for histological analysis. All skin specimens were frozen at −20 °C and fixed with the aid of Jung tissue freezing medium® (Leica, Germany). Following fixation, vertical sections of skin with a thickness of 5 μm were produced using the cryostat (CM 1850 UV, Leica, Germany) and collected on glass slide. The fat content of microtomed samples was removed using xylene with subsequent cleaning and dehydration by ethanol. The samples were then subjected to haematoxylin and eosin or van Gieson staining and observed under a light microscope (ProgRes C3, Leica, Germany). At least 5 replicates were conducted on each wound area and the representative sections were photographed.

2.13. Tensile strength

2.13.1. SCMC scaffold

The tensile strength at break of scaffolds was determined using a texture analyzer (Stable Micro System Ltd, Surrey, UK). The scaffold was cut into a rectangular shaped strip with 7.5 cm in length and 3.5 cm in width. It was mounted between upper and lower grips of analyzer. The pre-test speed, test speed, and withdrawal speed were fixed at 1.0, 0.5, and 0.5 mm/s respectively, with an acquisition rate of 200 points/min. Sample was uniaxially pulled with 30 kg loads. The maximum force to break was recorded. Triplicates were conducted and the results averaged.

2.13.2. Rat skin

The skin was harvested from rats receiving no dressing or treated with LV, MV and HV scaffolds after 30 days of experimentation. The furs on the healed region of wounded skin were shaved. The skin was cleansed with 0.9% (w/v) sodium chloride solution with the fat layers removed by means of a scalpel instead of organic solvent to avoid tissue distortion. The skin was cut into a strip of 5 cm in length and 2.5 cm in width. This strip was mounted between upper and lower grips of analyzer. The pre-test speed, test speed and withdrawal speeds were fixed at 5, 3, and 10 mm/s respectively,

with an acquisition rate of 200 points/min. Sample was uniaxially pulled with 30 kg loads. The maximum force to break was recorded unless otherwise stated. Triplicates were conducted and the results averaged.

2.14. Statistical analysis

All values were expressed in mean and standard deviation. The data were evaluated by Pearson correlation test, Student's *t*-test

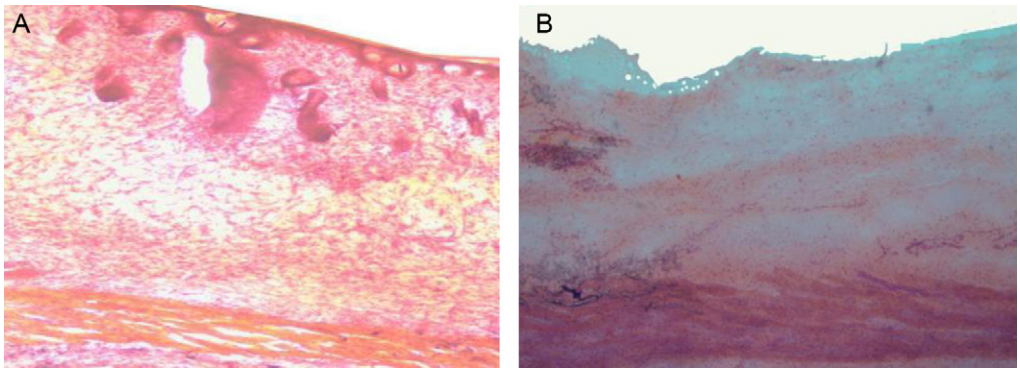

Fig. 1. Photomicrographs of H&E stained histology section for (a) normal skin and (b) partial thickness wounded skin.

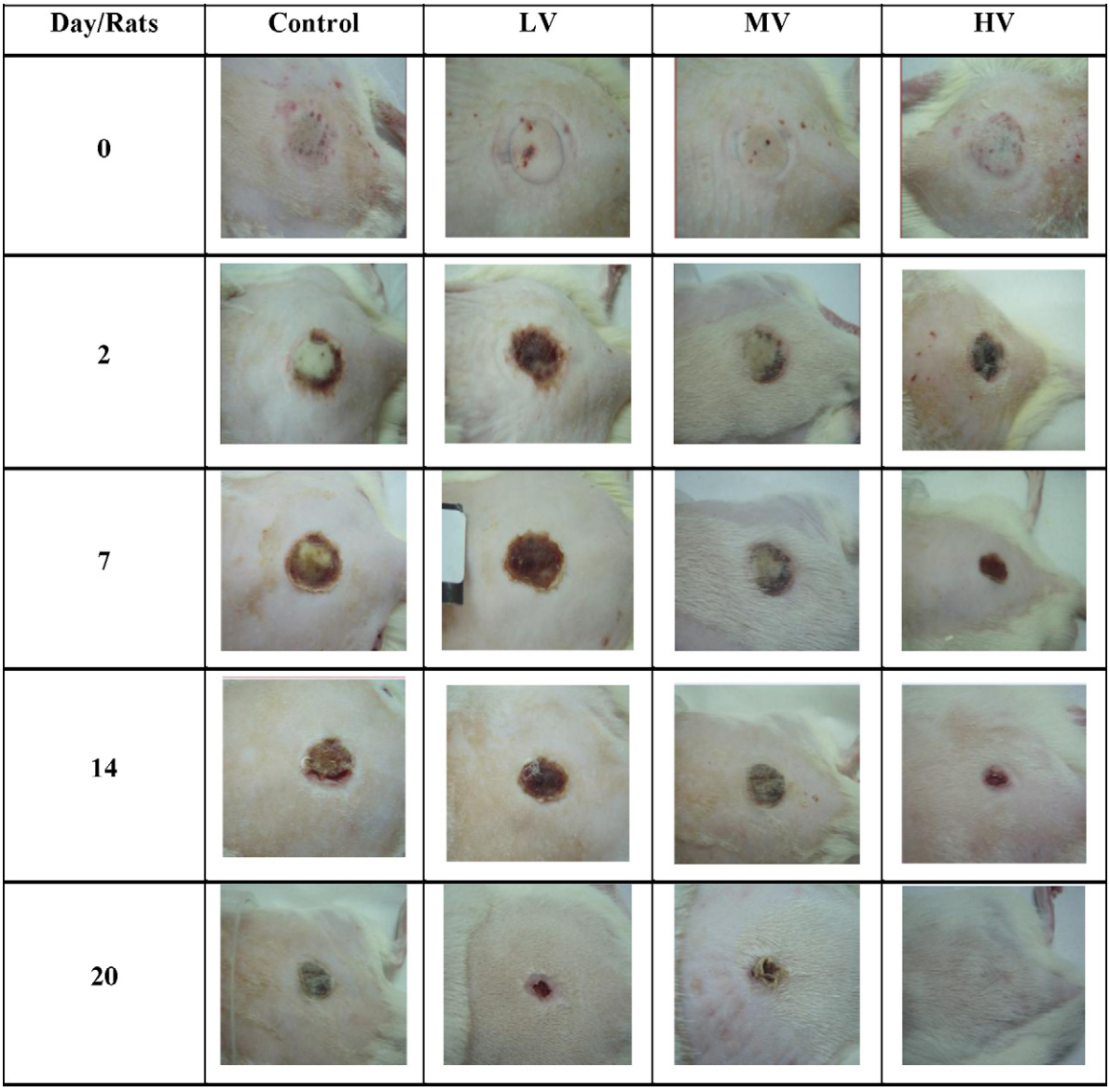

Fig. 2. Macroscopic wound images of rats with no applied scaffold (control) and treated by LV, MV and HV scaffolds.

or analysis of variance followed by post-hoc analysis. The level of significance was set at $p < 0.05$.

3. Results and discussion

3.1. Wound morphology

Fig. 1 shows that the rats were characterized by partial thickness wound. The entire epidermis and a variable fraction of dermis were destroyed by treating their dorsal abdominal skin with scalding water at 65 °C. The application of LV, MV and HV scaffolds accelerated the rate of wound healing. The size of wound was smaller and the propensity of re-epithelialization was higher in rats treated with SCMC scaffold than control (Figs. 2 and 3). The influence of SCMC scaffold on wound healing was similar to the recent findings of drug-free polyvinyl alcohol–chitosan hydrogel dressing particularly in case of wound size reduction (Sung et al., 2010). A smaller wound size in rats was noted with LV and MV scaffolds than control within the first 5 days of treatment (Fig. 3A, ANOVA: $p < 0.05$), and throughout 2 weeks when HV scaffold was used as dressing (Fig. 3A, ANOVA: $p < 0.05$).

At day 0 following the treatment of rats by scalding water, the skin demonstrated a white eschar with a hyperemic zone at the periphery of wound (Fig. 2). With time, the wound progressed from white eschar to a state of full hyperemia which indicated that the red blood cells undergoing extravasation. The rats treated with HV scaffold demonstrated a remarkably faster reduction in wound size and a higher re-epithelialization propensity than control and rats treated with LV or MV scaffold (Figs. 2 and 3, ANOVA: $p < 0.05$). These rats required 22 days to gain full re-epithelialization. A longer duration of 33 and 24 days were needed by control and rats treated with LV or MV scaffold in order to achieve the similar extent of re-epithelialization.

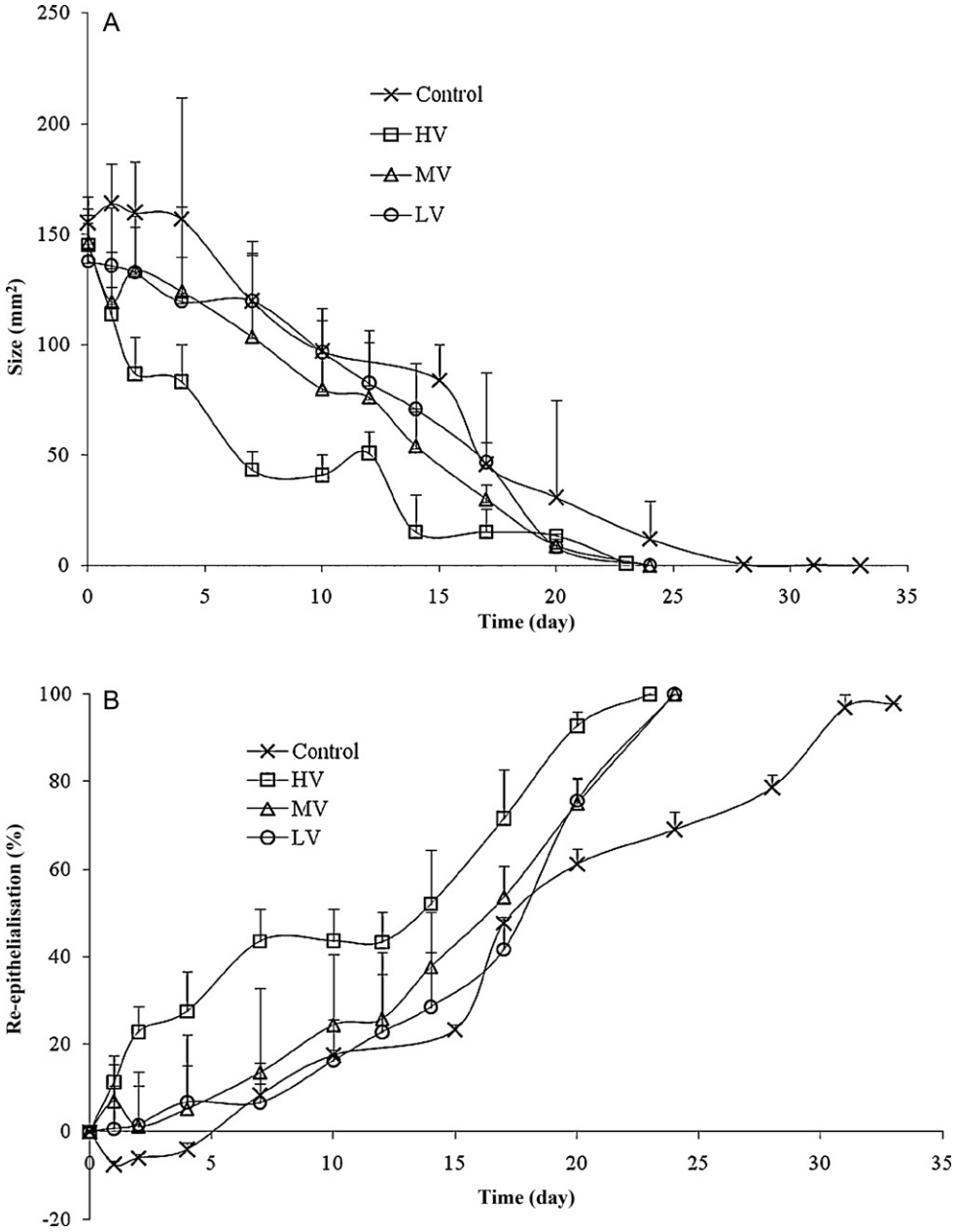

Fig. 3. Profiles of (a) wound size and (b) state of re-epithelialization of rats.

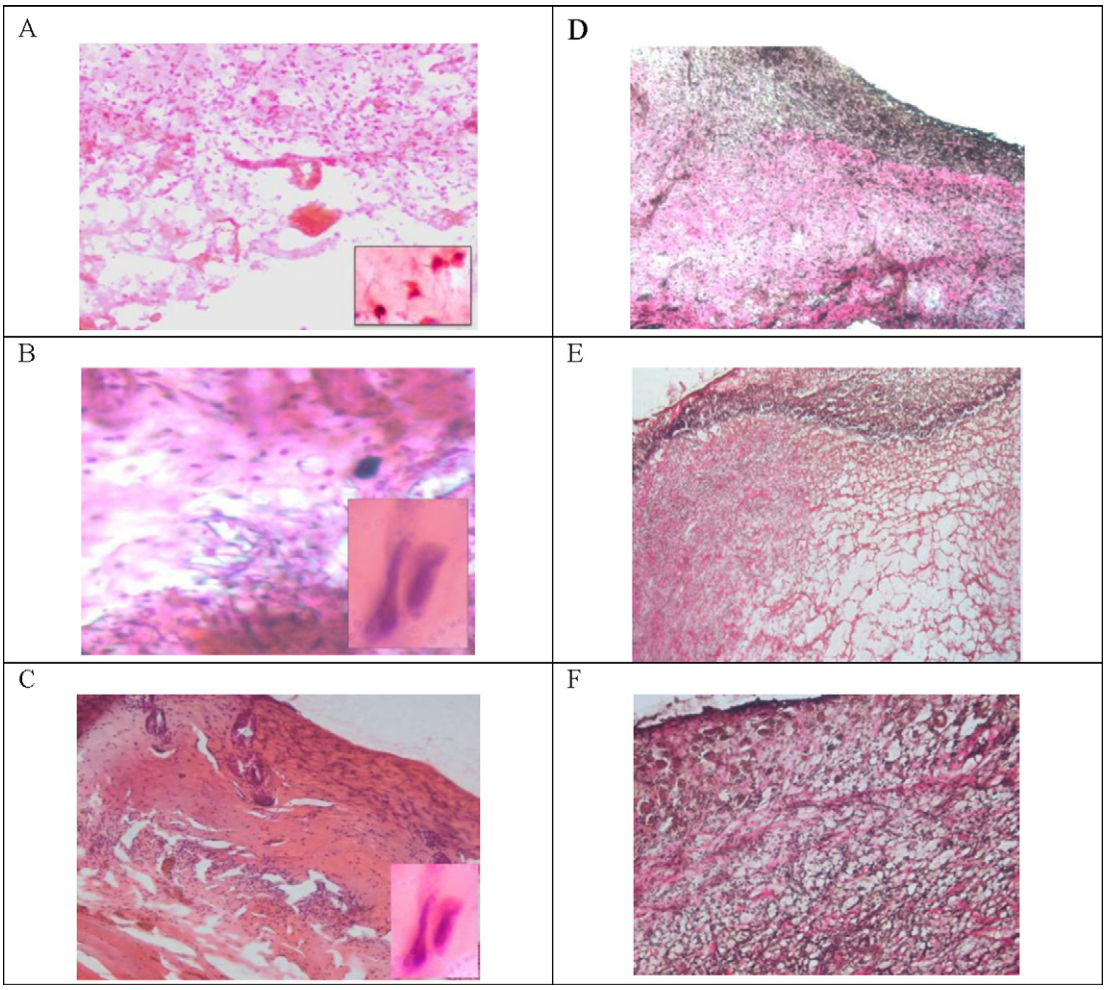

Fig. 4. Photomicrographs of H&E stained histology section for (a) control rat at day 2, (b) HV-treated rat at day 2, (c) HV-treated rat at day 7; van Giesons' stained histology section at day 14 for (d) control rat, (e) MV/LV-treated rats and (f) HV-treated rat.

Histology study using haematoxylin and eosin staining technique indicated that inflammatory responses with neutrophil and macrophage infiltration took place at the early phase of wound healing (Fig. 4A). At day 2 onwards, fibroblasts were identified in the tissue specimen (Fig. 4B and C). The macrophages were involved in activation of fibroblasts which were responsible for secretion of collagen, the main extracellular component of the skin (Kondo, 2007; Park and Barbul, 2004). The macrophages migrated into wound after injury before fibroblast migration and replication (Kondo, 2007). They secreted cytokines and growth factors, and regulated partly the fibroblast chemotaxis, proliferation as well as synthesis of glycoaminoglycans, proteoglycans and collagen of the new extracellular matrix (Tsirogianni et al., 2006). Van Gieson staining of tissue specimen obtained at day 14 indicated that a more homogeneous, closely packed and interwoven bundles of collagen (red-stained) and elastin (black-stained) fibres was noted in the wounded region of rats treated with HV scaffolds than MV or LV scaffolds and control (Fig. 4D–F). The form of matrix could affect the process of re-epithelialization (Ashcroft et al., 2002; Santoro and Gaudino, 2005; Tsirogianni et al., 2006) and these differences can lead to a faster rate of wound healing when HV scaffold was used in wound treatment. The collagen fibres are tough and resistant to stretching (Premkumar, 2004). Tensile strength analysis of wounded skins in rats treated with LV and MV scaffolds indicated that these skins were characterized by a tensile strength amounting to approximately 14 MPa (Table 1). The tensile strength of skin obtained from rats treated with HV scaffold was not determinable. This skin was resistant to be stretched under the given tensile load and was deemed to have a higher tensile strength than skin treated by LV and MV scaffolds.

3.2. Transepidermal water loss

TEWL refers to outward diffusion of water through skin (Levin and Maibach, 2005). Its measurement is used to gauge the moisture retention function of skin. The TEWL of rats was reduced when the scaffold was applied onto wound (Fig. 5, ANOVA: $p < 0.05$). The rats with wounded region treated with SCMC scaffold were

Table 1
Physicochemical characteristics of rat skin, SCMC and its scaffolds.

	LV	MV	HV
Polymer molecular weight (g/mol)	$7.2571 \times 10^5 \pm 1.1246 \times 10^4$	$2.8242 \times 10^6 \pm 3.2712 \times 10^4$	$6.4442 \times 10^6 \pm 2.9769 \times 10^5$
Polymer carboxymethyl substitution degree	1.1680 ± 0.0869	0.9004 ± 0.2268	1.3424 ± 0.0897
Scaffold tensile strength (MPa)	53.1310 ± 5.4840	57.9570 ± 6.0210	68.4030 ± 0.4120
Scaffold treated-skin tensile strength (MPa)	14.1550 ± 3.2970	14.2890 ± 2.0500	–

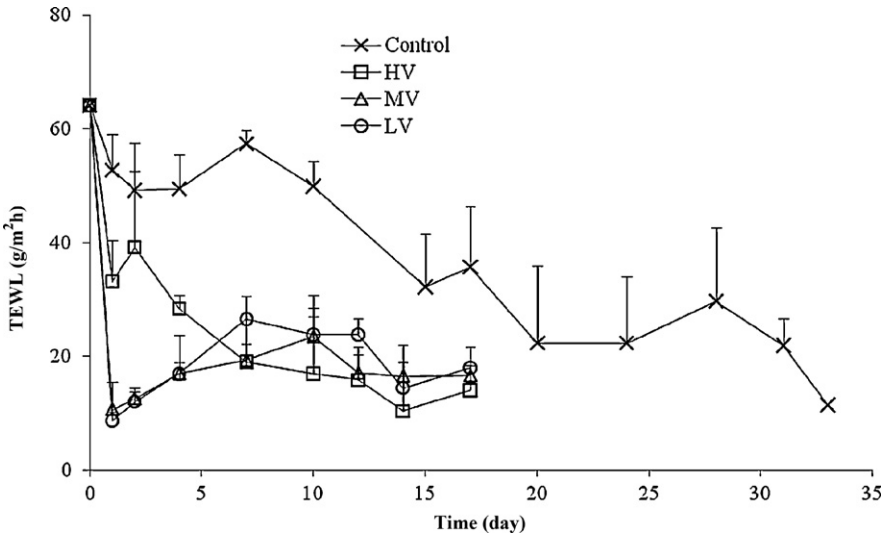

Fig. 5. Profiles of TEWL of rats with no applied scaffold (control) and treated by LV, MV and HV scaffolds.

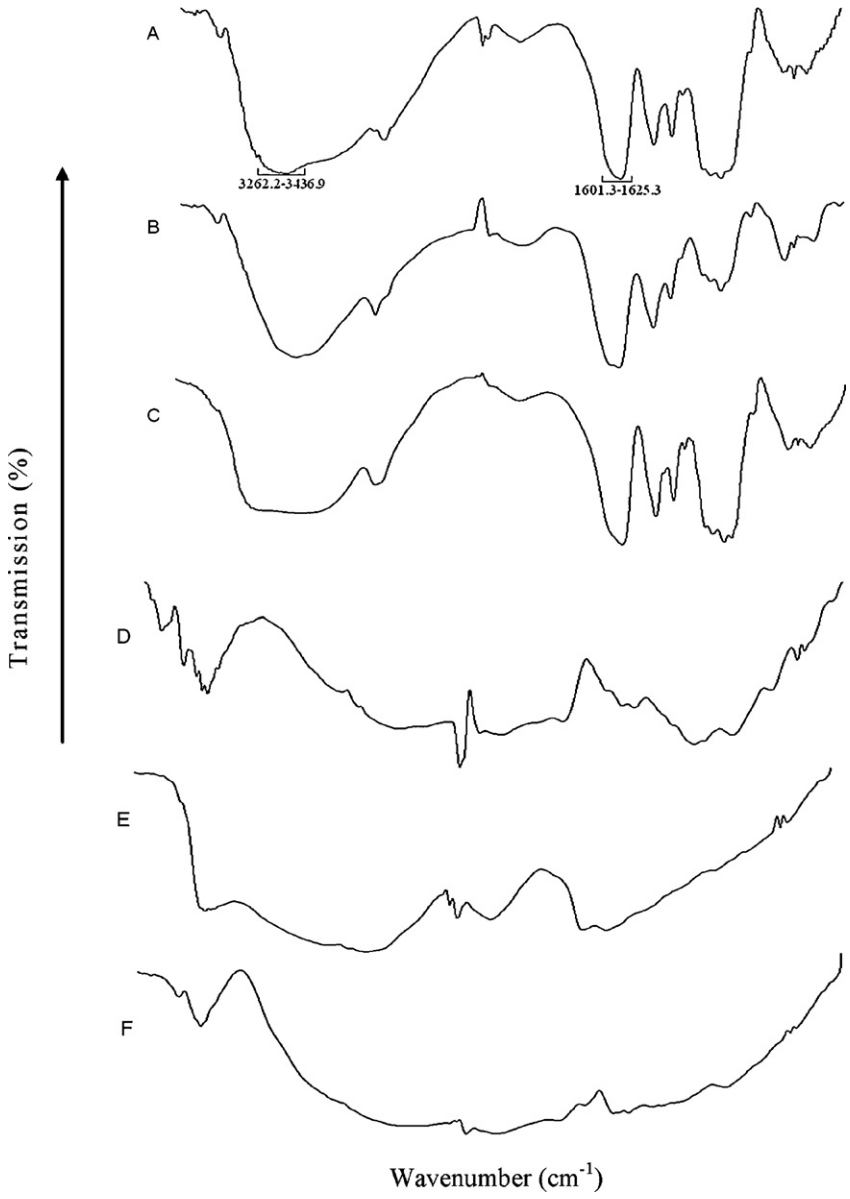

Fig. 6. FTIR spectra for (a) unprocessed LV, (b) unprocessed MV, (c) unprocessed HV, (d) LV Scaffold, (e) MV scaffold and (f) HV scaffold.

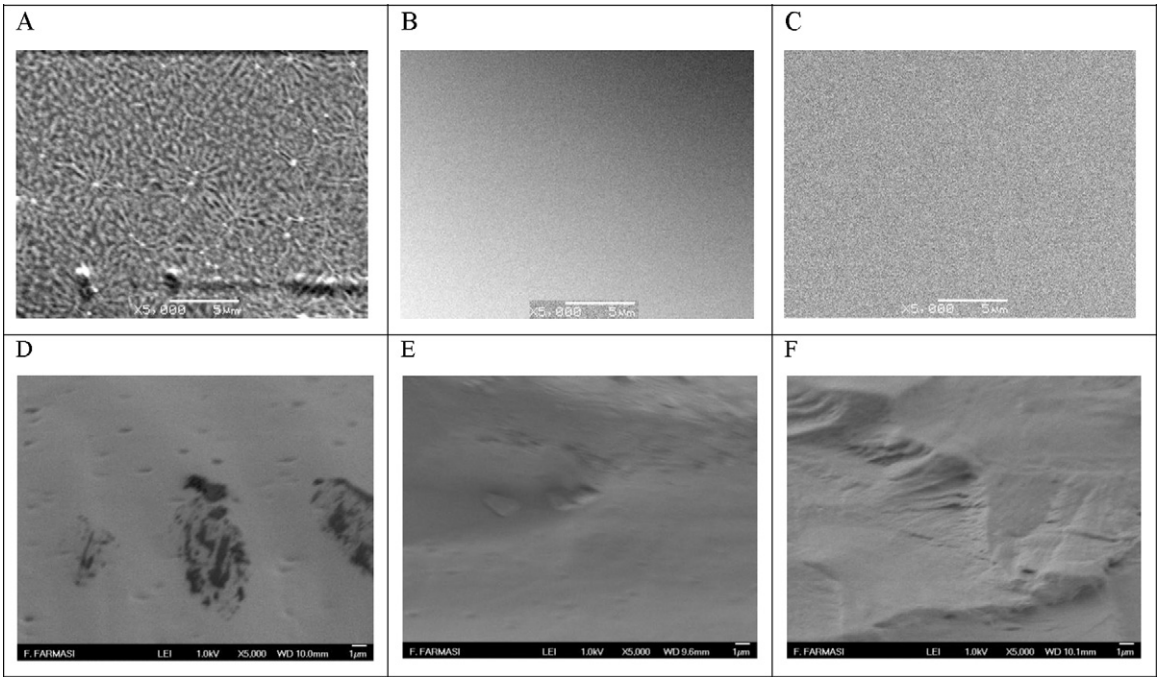

Fig. 7. SEM surface morphology of (a) LV scaffold, (b) MV scaffold, (c) HV scaffold, and cross-sectional morphology of (d) LV scaffold, (e) MV scaffold and (f) HV scaffold.

found to experience a faster healing rate owing to moisture retention at wound bed (Williams, 1999). In the absence of scaffold, the propensity of TEWL from wound of rats was high due to breakdown of epithelial barrier and fluid migration from blood capillary to extravascular tissues. In rats receiving no dressing, approximately 30 days were required to reduce their propensity of TEWL to a baseline similar to those treated with SCMC scaffold, through gradual healing of wound (Fig. 5).

Both LV and MV scaffolds negated the propensity of TEWL to a higher degree than HV scaffold within the first 7 days of application (Fig. 5, ANOVA: $p < 0.05$). Unlike control which exhibited excessive TEWL, the rats treated with LV or MV scaffold experienced excessive moisture retention. Excessive TEWL in control and moisture retention in rats treated with LV or MV scaffold translated to reduced cellular migration or attachment respectively. This can adversely affect the formative process of extracellular matrix and progress of wound healing (Bishop et al., 2003; Cutting and White, 2002; Field and Kerstein, 1994; Winter, 1962). The HV scaffold reduced the TEWL to an intermediate level. It could provide an optimal moist condition at wound bed during the initial period which was characterized by inflammation, migration and extracellular matrix synthesis. Consequently, the HV scaffold brought about a remarkably higher rate of wound healing than control and rats treated with LV or MV scaffold.

3.3. Physicochemical characteristics of scaffolds

FTIR analysis showed that the state of polymer–polymer interaction in LV, MV and HV scaffolds was high. This was indicated by FTIR spectra of scaffolds which were represented by broad bands between wavenumber regime of 400 and 4000 cm^{-1}, unlike sharp peaks demonstrated by matrices prepared from cellulose-based polymer and carboxylate-rich sodium alginate (Fig. 6) (Anuar et al., 2007; Ashikin et al., 2010; Wong et al., 2007). Among all matrices, the LV scaffold had the lowest tensile strength (Table 1). The scanning electron microscopy test indicated that macropores with pore size greater than 1 μm were present in LV scaffold (Fig. 7). The pores of LV scaffold displayed a micellar arrangement of polymer chains. This was probably due to LV had a shorter chain length than MV and HV which then granted systematic aggregation of LV molecules (Table 1, Student's *t*-test: $p < 0.05$). The MV and HV scaffolds had higher tensile strength values than LV scaffold (Table 1, ANOVA: $p < 0.05$). The MV and HV had larger molecular weights than LV. Random entanglement of polymer chains resulted in strong physical binding and the formation of extremely small nanopores (Fig. 7), beyond the detection by measurement tools such as scanning electron microscopy and mercury porosimetry techniques (Fan et al., 2009). The strong assembly of MV and HV in a scaffold was also reflected by their resistance to erode in USP phosphate buffer pH 7.4 after 12 h of immersion, in contrast to LV scaffold which completely dissolved in the same medium. High molecular weight SCMC has been reported to undergo a low interpenetration level between polymer and mucin molecules as a result of its entangled structure, low mobility and flexibility of polymer chains (Rossi et al., 1996). The resistance of high molecular weight HV scaffold to dissolve in simulated wound fluid suggested that the wound healing of rats can be brought about by physical regulation of TEWL instead of chemical-induced biological responses. It indicated that the HV scaffold can be placed closely to the surfaces of wound without ingrowth and disturbance of healing wound bed during treatment, similar to the observations reported by Vloemans et al. (2001).

The initial moisture content of LV, MV and HV scaffolds varied between 2.47 and 2.82% and was not significantly different from each other (Student's *t*-test: $p > 0.05$). In a water uptake capacity test using USP phosphate buffer pH 7.4 as the simulated wound medium, HV scaffold demonstrated a lower level of water uptake than MV scaffold, and the LV scaffold tended to absorb water, disintegrate and dissolve making an accurate assessment of its water uptake impossible (Fig. 8A, HV vs MV scaffold: ANOVA: $p < 0.05$). The higher affinity of LV scaffold for moisture than HV scaffold was also inferred in a separate test on their moisture adsorption profiles (Fig. 8B). The TEWL propensity of HV scaffold was high in spite of it had remarkably small pore characteristics (Fig. 7). The water movement can be fairly insensitive to the pore characteristics of a matrix (Xiong et al., 1992). The higher degree of TEWL from HV than LV

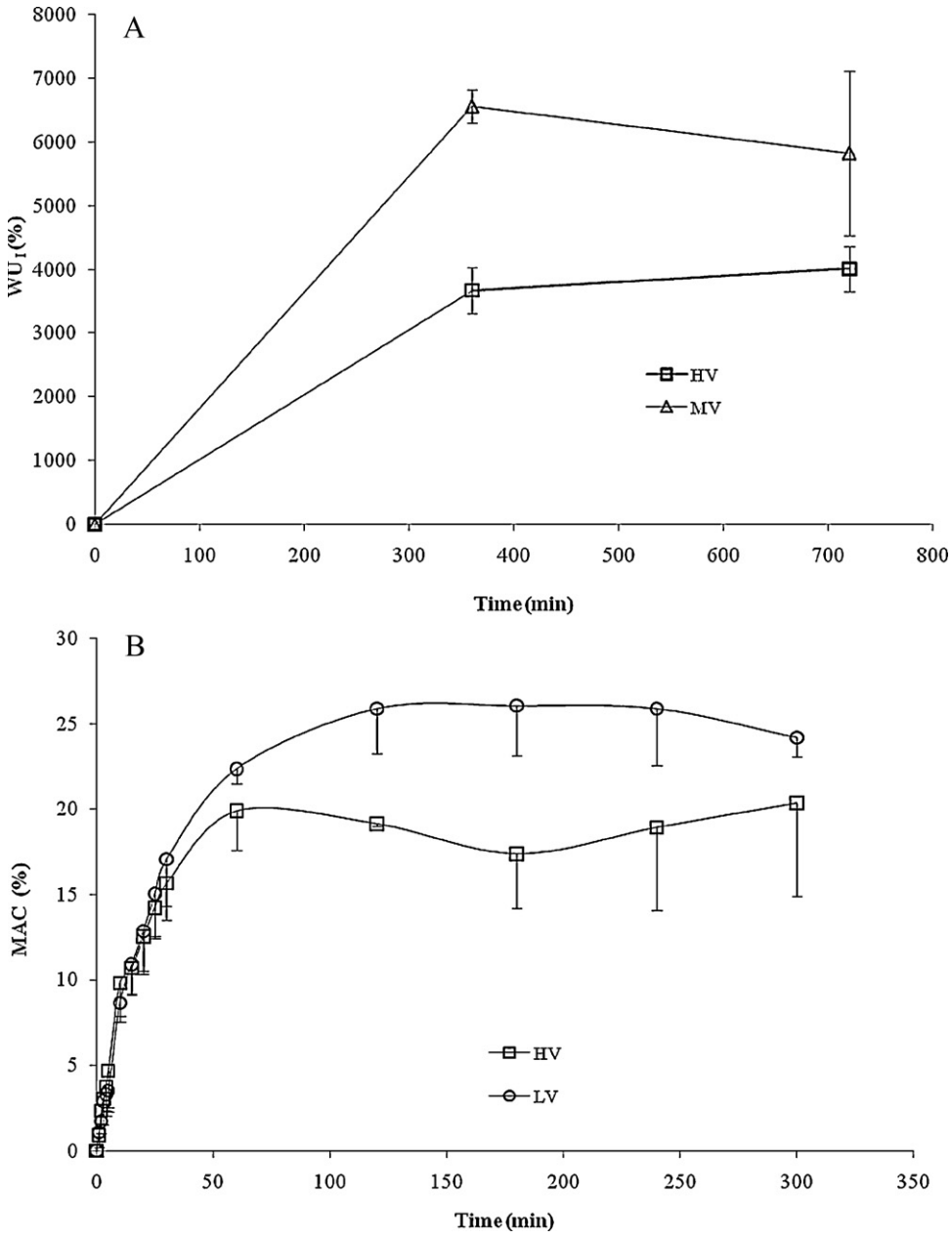

Fig. 8. Profiles of (a) water uptake and (b) moisture adsorption capacity of scaffolds.

or MV scaffold was ascribed to its lower affinity for moisture and reduced retention of moisture in matrix.

Pearson correlation study on the relationship between TEWL-time plot $AUC_{0-7\ days}$, SCMC molecular weight and its degree of carboxymethyl substitution indicated that the polymer molecular weight ($r = 0.972$, $p = 0.075$) had a stronger bearing on TEWL than degree of side chain substitution ($r = 0.710$, $p = 0.249$). The extent of TEWL was largely governed by SCMC molecular weight instead of its degree of carboxymethyl substitution. The HV had a larger molecular weight than LV and MV (Table 1). Its scaffold induced a higher propensity of TEWL in spite of HV exhibiting a similarly high degree of carboxymethyl substitution as LV (Table 1).

4. Conclusion

High molecular weight SCMC scaffold promoted a faster wound healing on the burn region of rats than lower molecular weight samples or control through optimal regulation of transepidermal water loss from wound. The propensity of transepidermal water loss from the wound regime of rats treated by control > HV scaffold > LV–MV scaffold. The HV scaffold can protect moisture loss without its excessive accumulation at the wound bed. The regulation of transepidermal water loss by scaffold is largely affected by the choice of polymer molecular weight instead of its carboxymethyl substitution degree or pore size distribution of matrix.

Acknowledgements

The authors wish to thank Ministry of Science, Technology and Innovation, and Ministry of Higher Education, Malaysia for funding (0141903) and facility support.

References

Anuar, N.K., Wong, T.W., Ghodgaonkar, D.K., Taib, M.N., 2007. Characterization of hydroxypropylmethylcellulose films using microwave non-destructive testing technique. J. Pharm. Biomed. Anal. 43, 549–557.

Ashcroft, G., Mills, S., Ashworth, J., 2002. Ageing and wound healing. Biogerontology 3, 337–345.
Ashikin, W.H.N.S., Wong, T.W., Law, C.L., 2010. Plasticity of hot air-dried mannuronate- and guluronate-rich alginate films. Carbohydr. Polym. 81, 104–113.
Bishop, S.M., Walker, M., Rogers, A.A., Chen, W.Y.J., 2003. Importance of moisture balance at the wound-dressing interface. J. Wound Care 12, 125–128.
Caruso, D.M., Foster, K.N., Hermans, M.H.E., Rick, C., 2004. Aquacel Ag® in the management of partial-thickness burns: results of a clinical trial. J. Burn Care Res. 25, 89–97.
Cutting, K.F., White, R.J., 2002. Maceration of the skin and wound bed 1: its nature and causes. J. Wound Care 11, 275–278.
Czaja, W., Krystynowicz, A., Bielecki, S., Brown, J.R.M., 2006. Microbial cellulose—the natural power to heal wounds. Biomaterials 27, 145–151.
D'Hemecourt, P.A., Smiell, J.M., Karim, M.R., 1998. Sodium carboxymethylcellulose aqueous-based gel vs. Becaplermin gel in patients with nonhealing lower extremity diabetic ulcers. Wounds 10, 69–75.
Fan, X.J., Lee, S.W.R., Han, Q., 2009. Experimental investigations and model study of moisture behaviors in polymeric materials. Microelectron. Reliab. 49, 861–871.
Field, C.K., Kerstein, M.D., 1994. Overview of wound healing in a moist environment. Am. J. Surg. 167, 6.
Guo, J.-H., Skinner, G.W., Harcum, W.W., Barnum, P.E., 1998. Pharmaceutical applications of naturally occurring water-soluble polymers. Pharm. Sci. Technol. Today 1, 254–261.
Huang, M.-H., Yang, M.-C., 2008. Evaluation of glucan/poly(vinyl alcohol) blend wound dressing using rat models. Int. J. Pharm. 346, 38–46.
Huang, S.-H., Yang, P.-S., Wu, S.-H., Chang, K.-P., Lin, T.-M., Lin, S.-D., et al., 2010. Aquacel® ag with vaseline gauze in the management of toxic epidermal necrolysis. Burns 36, 121–126.
Kamer, E., Unalp, H., Tarcan, E., Diniz, G., Atahan, K., Ortac, R., et al., 2008. Effect of hyaluronic acid–carboxymethylcellulose adhesion barrier on wound healing: an experimental study. Wounds 20, 7.
Karathanos, V.T., Saravacos, G.D., 1993. Porosity and pore size distribution of starch materials. J. Food Eng. 18, 259–280.
Kondo, T., 2007. Timing of skin wounds. Leg. Med. 9, 109–114.
Kulicke, W.-M., Kull, A.H., Kull, W., Thielking, H., Engelhardt, J., Pannek, J.-B., 1996. Characterization of aqueous carboxymethylcellulose solutions in terms of their molecular structure and its influence on rheological behaviour. Polymer 37, 2723–2731.
Levin, J., Maibach, H., 2005. The correlation between transepidermal water loss and percutaneous absorption: an overview. J. Control. Release 103, 291–299.
Liu, L., Liu, D., Wang, M., Du, G., Chen, J., 2007. Preparation and characterization of sponge-like composites by cross-linking hyaluronic acid and carboxymethylcellulose sodium with adipic dihydrazide. Eur. Polym. J. 43, 2672–2681.
Ludwig, A., 2005. The use of mucoadhesive polymers in ocular drug delivery. Adv. Drug Deliv. Rev. 57, 1595–1639.
Park, J.E., Barbul, A., 2004. Understanding the role of immune regulation in wound healing. Am. J. Surg. 187, S11–S16.
Piaggesi, A., Baccetti, F., Rizzo, L., Romanelli, M., Navalesi, R., Benzi, L., 2001. Sodium carboxyl-methyl-cellulose dressings in the management of deep ulcerations of diabetic foot. Diabet. Med. 18, 320–324.
Premkumar, K. (Ed.), 2004. The Message Connection: Anatomy and Physiology, 2nd ed. Lippincott Williams and Wilkins, U.S.A..
Rossi, S., Bonferoni, M.C., Ferrari, F., Bertoni, M., Caramella, C., 1996. Characterization of mucin interaction with three viscosity grades of sodium carboxymethylcellulose. Comparison between rheological and tensile testing. Eur. J. Pharm. Sci. 4, 189–196.
Santoro, M.M., Gaudino, G., 2005. Cellular and molecular facets of keratinocyte reepithelization during wound healing. Exp. Cell Res. 304, 274–286.
Sebert, P., Bourny, E., Rollet, M., 1994. Gamma irradiation of carboxymethylcellulose: technological and pharmaceutical aspects. Int. J. Pharm. 106, 103–108.
Sudhakar, Y., Kuotsu, K., Bandyopadhyay, A.K., 2006. Buccal bioadhesive drug delivery a promising option for orally less efficient drugs. J Control. Release 114, 15–40.
Sung, J.H., Hwang, M.-R., Kim, J.O., Lee, J.H., Kim, Y.I., Kim, J.H., Chang, S.W., Jin, S.G., Kim, J.A., Lyoo, W.S., Han, S.S., Ku, S.K., Yong, C.S., Choi, H.-G., 2010. Gel characterisation and *in vivo* evaluation of minocycline-loaded wound dressing with enhanced wound healing using polyvinyl alcohol and chitosan. Int. J. Pharm. 392, 232–240.
Tsirogianni, A.K., Moutsopoulos, N.M., Moutsopoulos, H.M., 2006. Wound healing: immunological aspects. Injury 37, S5–S12.
Vloemans, A.F.P.M., Soesman, A.M., Kreis, R.W., Middelkoop, E., 2001. A newly developed hydrofibre dressing, in the treatment of partial-thickness burns. Burns 27, 167–173.
Wang, M., Xu, L., Hu, H., Zhai, M., Peng, J., Nho, Y., et al., 2007. Radiation synthesis of pvp/cmc hydrogels as wound dressing. Nucl. Instrum. Methods Phys. Sect. B 265, 385–389.
Williams, C., 1999. An investigation of the benefits of aquacel hydrofibre wound dressing. Br. J. Nursing 8, 676–680.
Winter, G.D., 1962. Formation of the scab and the rate of epithelization of superficial wounds in the skin of the young domestic pig. Nature 193, 293–294.
Wong, T.W., Deepak, K.G., Taib, M.N., Anuar, N.K., 2007. Microwave non-destructive testing technique for characterization of HPMC-PEG 3000 films. Int. J. Pharm. 343, 122–130.
Xiong, X., Narsimhan, G., Okos, M.R., 1992. Effect of composition and pore structure on binding energy and effective diffusivity of moisture in porous food. J. Food Eng. 15, 187–208.